Brief Articles

N-{3-[2-(4-Alkoxyphenoxy)thiazol-5-yl]-1-methylprop-2-ynyl}carboxy Derivatives as Acetyl-CoA Carboxylase Inhibitors—Improvement of Cardiovascular and Neurological Liabilities via Structural Modifications

Yu Gui Gu,*,† Moshe Weitzberg,† Richard F. Clark,† Xiangdong Xu,† Qun Li,† Nathan L. Lubbers,‡ Yi Yang,§ David W. A. Beno,|| Deborah L. Widomski,‡ Tianyuan Zhang,† T. Matthew Hansen,† Robert F. Keyes,† Jeffrey F. Waring,§ Sherry L. Carroll,|| Xiaojun Wang,† Rongqi Wang,† Christine H. Healan-Greenberg,§ Eric A. Blomme,§ Bruce A. Beutel,† Hing L. Sham,† and Heidi S. Camp†

Global Pharmaceutical Research and Development, Abbott Laboratories, 200 Abbott Park Road, Abbott Park, Illinois 60064

Received January 10, 2007

A preliminary safety evaluation of ACC2 inhibitor **1**-(*S*) revealed serious neurological and cardiovascular liabilities of this chemotype. A systematic structure−toxicity relationship study identified the alkyne linker as the key motif responsible for these adverse effects. Toxicogenomic studies in rats showed that **1**-(*R*) and **1**-(*S*) induced gene expression patterns similar to that seen with several known cardiotoxic agents such as doxorubicin. Replacement of the alkyne with alternative linker groups led to a new series of ACC inhibitors with drastically improved cardiovascular and neurological profiles.

Introduction

The increasing epidemic of type 2 diabetes in recent years is largely attributed to proliferation of key risk factors, which include a high fat diet, a sedentary lifestyle, and the demographic shift to a more aged population. It is well accepted that increased abdominal obesity and physical inactivity contribute significantly to the development of type 2 diabetes. It is estimated that approximately 80% of type 2 diabetics are considered obese in Western societies.[1,2]

The pathophysiology of obesity-induced diabetes initiates when the ability of adipose tissue to store excess nutrients exceeds its capacity due to increased energy intake. At the cellular level, this leads to an increase in ectopic fat accumulation in nonadipose tissues such as skeletal muscle, liver, and pancreas. It has been shown that the level of intracellular lipids found in skeletal muscle and liver is a strong predictor of the development of insulin resistance and type 2 diabetes.[3,4] Therefore, there has been increasing research interest in the paradigm of altering lipid disorders by targeting enzymes that are involved in lipid synthesis and oxidation.[5]

Acetyl-CoA carboxylases[6] (ACC[a]) play an important role in lipid pathways via the modulation of malonyl Co-A (mCoA),[7,8] a key regulator of fatty acid metabolism. ACC1, a 265 kDa cytosolic protein, is primarily expressed in lipogenic tissues (liver and adipose),[9] whereas ACC2, a 280 kDa protein located in the mitochondrial outer membrane, is highly expressed in oxidative tissues (muscle, heart, and liver).[10] Genetic studies have demonstrated that ACC1 knockout in mouse is embryonically lethal,[11] whereas ACC2 homozygous mice are healthy, fertile, and have a higher fatty acid oxidation rate and reduced fat accumulation compared to their wild type cohorts.[12,13] Recently, we reported a class of novel ACC inhibitors exemplified by **1**-(*S*) (Figure 1).[14] **1**-(*S*) is a potent and selective ACC2 inhibitor with an ACC2 IC_{50} of 38 nM and >1000-fold selectivity against ACC1. This compound has also demonstrated dose-dependent mCoA lowering in muscles of rodents with minimal effect on mCoA levels in liver in an acute setting, consistent with results observed for ACC2 homozygous knockout mice.[12]

Recently, our colleagues at Abbott demonstrated that an acute anesthetized rat cardiovascular model is an effective tool to identify compounds with undesirable cardiovascular and neurological liabilities at an early stage of lead optimization,[15,16] and it has been successfully applied to triage melanin-concentrating hormone receptor 1 antagonists based on cardiovascular safety profiles.[17] We utilized this rat cardiovascular model to preliminarily evaluate the safety profiles of our ACC2 inhibitors. A hemodynamic study of **1**-(*S*) in anesthetized rats using intravenous dosing revealed serious seizure and cardiovascular liabilities. We reasoned that because ACC2 knockout mice have been reported to be healthy and behave normally, the observed toxic effects of **1**-(*S*) are likely associated with the chemical structure of this compound, rather than a result of ACC2 inhibition. Compounds **5a** and **5b**, two structurally related yet inactive analogues, provided initial support for this hypothesis. These compounds caused seizures in anesthetized rats at 45 mg/kg and 15 mg/kg, respectively (Table 1). This result prompted a systematic screen of more than twenty compounds containing structural variations in different areas of the molecule to identify the structural motif responsible for the cardiovascular and neurological side effects.

Chemistry

As reported previously,[14] the alkyne derivatives **5** were synthesized from **2** via Sonogashira coupling with **4**, followed by deprotection of the phthalimide group and derivatization of

* To whom correspondence should be addressed. Tel.: (847) 937-4792. Fax: (847) 938-3403. E-mail: yu-gui.y.gu@abbott.com.
† Metabolic Disease Research.
‡ Integrative Pharmacology.
§ Cellular, Molecular, and Exploratory Toxicology.
|| Exploratory Kinetics.
[a] Abbreviations: ACC, acetyl-CoA carboxylase; mCoA, malonyl-CoA.

10.1021/jm070035a CCC: $37.00
Published on Web 02/14/2007

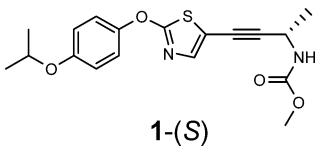

1-(*S*)

Figure 1. Selective ACC2 inhibitor.

the resulting primary amine (Scheme 1). Lithiation of **3**, which was synthesized by reacting 4-isopropoxyphenol with 2-bromothiazole, and subsequent reaction with *N*-formylmorpholine produced **6**. Compound **6** was sequentially reacted with hydroxylamine and *N*-chlorosuccinimide (NCS) to provide the corresponding chloroaldoxime, which upon treatment with base underwent [3+2] dipolar cycloaddition with alkyne **4** to provide **8** regioselectively. Compound **8** was readily converted to **9**, as depicted in Scheme 1. Alternatively, the anion derived from **3** was reacted with tributyltin chloride to provide stannane **7**. Stille coupling of **7** with 2-bromothiazole yielded dithiazole compound **10**. Lithiation of the terminal thiazole with *n*-BuLi and treatment of the resulting anion with acetaldehyde gave alcohol **11**. Compound **11** was converted to **12** by following a modified Ritter reaction condition.[18]

Hemodynamic Studies in Rats

Hemodynamic studies in anesthetized rats were carried out to evaluate the preliminary cardiovascular and neurological safety of ACC2 inhibitors without knowing accurate efficacious drug concentrations. A screening protocol was established whereby compound administration was incrementally increased via 30-minute intravenous infusions at doses of 4.5, 15, and 45 mg/kg to achieve a targeted maximum plasma drug concentration of approximately 90 μg/mL based on the solubility with the current series.

Racemic analogues of **1** were screened to quickly identify any structure motif(s) in the current series, which might be associated with observed side effects. Variations at both termini of the molecule did not improve neurological properties in the series. Introduction of isopropoxy replacements such as cyclopropylmethoxy and cyclopropylmethylamino at the left-hand hydrophobic terminus also produced seizure activity (Table 1, **5c** vs **5d** and **5e**). Similarly, the incorporation of functionalities such as amide, methyl carbamate, and methylurea at the right-hand polar end of the molecule did not alter seizure toxicity profiles (Table 1, **5c**, **5f**−**i**). Improvement of the neurological toxicity profile was finally achieved when the alkyne moiety was replaced with other linker groups such as five-membered heteroaryls. Isoxazolyl (**9**) and thiazolyl (**12**) analogues exhibited no seizure effects in the anesthetized rat model (Table 1). These results indicate that the alkyne linker is responsible for neurological toxicity within the series.

In addition to neurological toxicity, some of the ACC2 inhibitors in the alkyne series also exhibited adverse cardiovascular events. Compound **5c**, for example, showed a large, time-dependent increase (47%) in cardiac contractility (dP/dt) (Figure 2A). It has been satisfying to discover that replacement of the alkyne linker with a five-membered heteroaryl group not only improves neurological toxicity profiles, but also dramatically enhances cardiovascular safety. Compound **9**, a direct nonalkynyl analogue of **5c**, showed no adverse cardiovascular events after escalating intravenous dosing up to 45 mg/kg (Figure 2B). Similar results were observed with other alkynyl/nonalkynyl compound pairs (data not shown). Whether the seizure and adverse cardiovascular effects are interrelated or caused by independent mechanisms is unknown.

Gene Expression

The results of the rat cardiovascular study prompted us to evaluate the effects of various ACC inhibitors on cardiac gene expression patterns. Male Sprague−Dawley rats were treated orally with active (*S*) and inactive (*R*)[14] enantiomers of **1** and **9**, respectively, at 100 mg/kg b.i.d dosing for 3 days. Compounds **9**-(*R*) and **9**-(*S*) have virtually identical oral pharmacokinetic profiles in rat (see Supporting Information). Compound **9**-(*S*) is a very potent ACC inhibitor with hACC1 $IC_{50} = 0.020$ μM and hACC2 $IC_{50} = 0.003$ μM, while **9**-(*R*) is a very weak ACC inhibitor (hACC1 $IC_{50} = 3.35$ μM and hACC2 $IC_{50} = 0.63$ μM). Doxorubicin, an anticancer drug known to induce cardiotoxicity, was used as a positive control.[19] No changes were observed in serum chemistry parameters or heart histology, other than mild cholesterol elevation in rats treated with active enantiomers **1**-(*S*) and **9**-(*S*), respectively. Gene expression profiles in heart were generated using the Affymetrix RAE230A microarray platform and were subjected to principal component analysis, in which the position of the points in space reflects integrated gene expression profiles derived from each treatment. As shown in Figure 3A, the gene expression patterns induced by both (*R*)- and (*S*)-enantiomers of **1** were similar to those induced by doxorubicin, clearly separating from patterns induced by the active and inactive enantiomers of **9**.

The gene expression changes were also compared to those present in the Iconix *DrugMatrix* database, which contains gene expression profiles of multiple organs of rats treated with over 600 known pharmacological and toxicological agents.[20] Figure 3B demonstrates the comparison of gene expression patterns induced by ACC inhibitors to that found in heart *DrugMatrix* database. Compound **1**-(*R*) had strong correlations with a number of reference expression profiles within *DrugMatrix*. The majority of these reference expression profiles are from known cardiotoxicants or cardiotonic agents, including doxorubicin, cyclosporine A, haloperidol, dobutamine, and norepinephrine. Compound **1**-(*S*), to a lesser extent, also had similar gene expression patterns to the known cardiotoxicants in *DrugMatrix*. In contrast, the gene expression profiles induced by **9**-(*S*) and **9**-(*R*) had little or no similarities to the known toxicants. Because the gene expression changes occurred for both the active and the inactive enantiomers of **1**, the observed cardiotoxicity is most likely independent of target inhibition.

We also evaluated gene expression changes related to various biological pathways. The alkynyl compounds **1**-(*S*) and **1**-(*R*) significantly impacted the expression levels of genes involved in mitochondrial oxidative phosphorylation pathway, such as NADH dehydrogenase (ubiquinone), ubiquinol-cytochrome c reductase, cytochrome c oxidase, and ATP synthase, in a similar fashion to the known cardiac toxicant doxorubicin, whereas the nonalkynyl compounds did not.

Conclusion

Structure−toxicity relationship studies found the alkyne moiety to be responsible for the observed neurological and cardiovascular adverse effects of our lead series of ACC2 inhibitors exemplified by **1**-(*S*). Gene expression profiles in heart tissues of rats treated with active and inactive enantiomers of **1** (**1**-(*S*) and **1**-(*R*), respectively) correlate to those of known cardiotoxicants. Replacement of the alkyne with alternative link groups such as heteroaryls dramatically reduces the cardiovascular and neurological liabilities of the series while maintaining ACC2 inhibitory activity. A full account of the SAR including the regain of ACC2 selectivity and pharmacological evaluation of this new series of compounds will be published separately.

Table 1. Neurological Liabilities of ACC Inhibitors[a]

#	Structure	hACC1 IC_{50} (μM) ± SEM	hACC2 IC_{50} (μM) ± SEM	Seizure[b]	plasma conc. (μg/mL)	B/P[c]
1-(*S*)	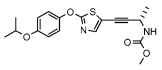	>30	0.038 ± 0.006	yes	75	1.7
5a	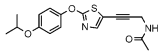	>30	1.73 ± 0.48	yes	81	1.1
5b	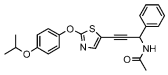	>30	>30	yes	32[d]	1.1
5c	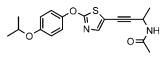	>30	0.019 ± 0.002	yes	72	ND[e]
5d	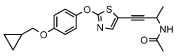	1.30 ± 0.89	0.007 ± 0.001	yes	31[d]	0.66
5e	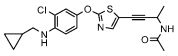	4.25 ± 1.42	0.014 ± 0.001	yes	201	0.69
5f	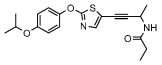	>30	0.047 ± 0.006	yes	8.3[d]	3.9
5g	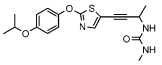	>30	0.032 ± 0.004	yes	42	0.69
5h	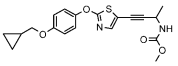	0.67 ± 0.14	0.026 ± 0.009	yes	43	2.1
5i	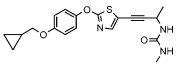	3.11 ± 2.73	0.009 ± 0.001	yes	43	1.1
9	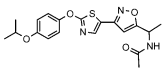	0.093 ± 0.002	0.008 ± 0.000	no	80	0.54
12	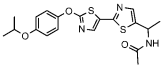	0.21 ± 0.01	0.028 ± 0.008	no	62	2.5

[a] The compound was administered in ascending 30 min intravenous infusions at doses of 4.5, 15, and 45 mg/kg in an attempt to reach a maximal plasma drug level of ~90 μg/mL, based on known solubility limitations. [b] The seizure activity was characterized by slight twitching of the limbs with progression to violent jerking of the head and torso. [c] Brain/plasma drug level ratio. [d] The study was terminated prematurely due to severe seizure. [e] Not determined.

Experimental Section

2-(4-Isopropoxyphenoxy)thiazole-5-carbaldehyde (6). To a solution of **3** (11.8 g, 0.05 mol) in dry THF was added *n*-BuLi (20 mL of 2.5 M solution, 0.05 mol) at −78 °C over 15 min. After 1 h, N-formylmorpholine (5.8 g, 0.05 mol) was added dropwise, and the mixture was stirred for 4 h and then quenched with satd NH_4Cl. The standard workup and purification on a silica gel flash column, eluting with 5~35% ethyl acetate in hexane, provided 13.2 g of **6** as a yellow oil (100% yield). ^{1}H NMR (300 MHz, $CDCl_3$) δ ppm 9.83 (s, 1H), 7.93 (s, 1H), 7.13−7.22 (m, 2H), 6.88−6.98 (m, 2H), 4.46−4.61 (m, 1H), 1.36 (d, J = 5.88 Hz, 6H). MS (ESI) *m*/*z*: 264.1 $(M + H)^+$.

2-(1-(3-(2-(4-Isopropoxyphenoxy)thiazol-5-yl)isoxazol-5-yl)-ethyl)isoindoline-1,3-dione (8). To a solution of **6** (2.5 g, 0.0095 mol) in pyridine (15 mL, 0.19 mol) was added hydroxylamine hydrochloride (6.6 g, 0.095 mol) portionwise, and the mixture was stirred at room temperature for 5 min and then heated at 70 °C for 0.5 h. Water (300 mL) was added, and the mixture was stirred for 20 min. The solid was filtered and dried to give 2.26 g of the corresponding oxime, which was dissolved in DMF and treated with NCS (1.17 g, 0.0085 mol). The mixture was stirred at room temperature for 6 h and water was added. The stirring was continued for an additional 30 min, and the precipitate was collected via filtration and dried to give 2.43 g of the chloroaldoxime as an off-white solid (82%).

To a solution of the chloroaldoxime (0.31 g, 0.001 mol) and **4** (R = Me, 0.2 g, 0.001 mol) in toluene was added potassium carbonate (0.42 g, 0.003 mol), and the reaction was heated at reflux for 6 h. After cooling to room temperature, the reaction mixture was diluted with methylene chloride and filtered. The filtrate was concentrated and purified on a silica gel flash column (eluting with 10~30% ethyl acetate in hexane) to give 0.33 g of **8** (70%). ^{1}H NMR (300 MHz, $CDCl_3$) δ ppm 7.82−7.94 (m, 2H), 7.69−7.80 (m, 2H), 7.53 (s, 1H) 7.14−7.24 (m, 2H), 6.85−6.97 (m, 2H), 6.51 (s, 1H), 5.67 (q, J = 7.35 Hz, 1H), 4.41−4.64 (m, 1H), 1.91 (d, J = 7.35 Hz, 3H), 1.35 (d, J = 5.88 Hz, 6H). MS (ESI) *m*/*z*: 476.0 $(M + H)^+$.

***N*-(1-(3-(2-(4-Isopropoxyphenoxy)thiazol-5-yl)isoxazol-5-yl)-ethyl)acetamide (9).** A mixture of **8** (3.9 g, 0.0082 mol) and hydrazine monohydrate (4.1 g, 0.082 mol) in 110 mL of methylene chloride/ethanol (10:1) was refluxed for 3 h. The mixture was cooled and filtered. The filtrate was concentrated, and the residue was suspended in methylene chloride and filtered again. The filtrate was concentrated to give 3.2 g of crude amine, which was dissolved

Scheme 1[a]

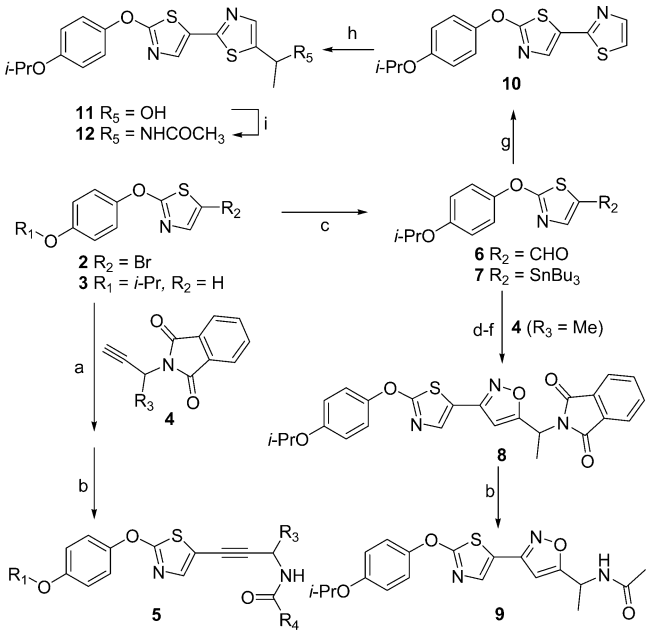

[a] Reagents and conditions: (a) $Pd(Ph_3P)_2Cl_2$ (5% equiv), CuI (2% equiv), Et_3N (5 equiv), THF, reflux, 3 h, 60−80%; (b) (i) NH_2NH_2 (10 equiv), CH_2Cl_2/EtOH (10:1), reflux, 3 h; (ii) Ac_2O (3 equiv) (or MeN═C═O for **5g**, **5i**; MeOCOCl for **1**, **5h**; and EtCOCl for **5f**), Et_3N (10 equiv), rt, 3 h, 35−81% (two steps); (c) BuLi (1.05 equiv), *N*-formylmorpholine (1.05 equiv) for **6** (or Bu_3SnCl for **7**), THF, −78 °C to rt, 87−93%; (d) NH_2OH·HCl (10 equiv), pyridine (20 equiv), rt to 70 °C, 95%; (e) NCS (1.0 equiv), DMF, rt 96%; (f) **4** (R_3 = Me), K_2CO_3 (3.0 equiv), toluene, relux, 70%; (g) 2-bromothiazole (0.95 equiv), $Pd(Ph_3P)_4$ (5% equiv), DMF, 60 °C, 95%; (h) BuLi (1.1 equiv), acetaldehyde (2.0 equiv), THF, −78 °C to rt, 83%; (i) BF_3·Et_2O (excess), CH_3CN, CH_2Cl_2, reflux, 35%.

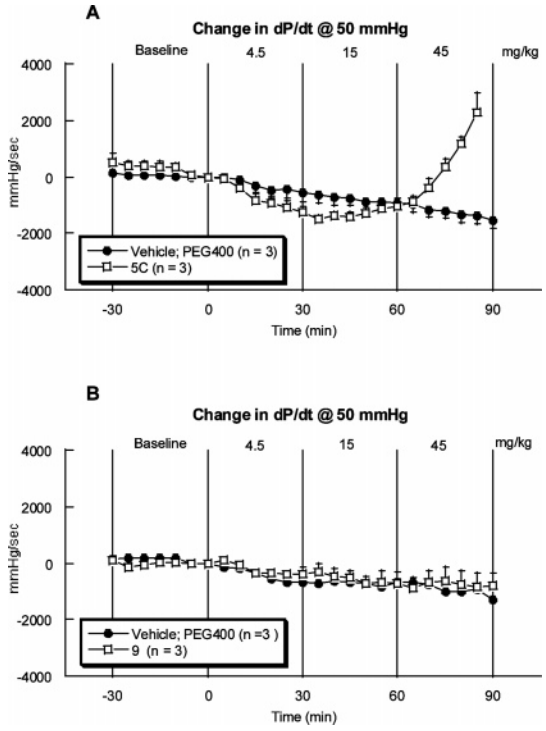

Figure 2. Cardiac contractility of **5c** (A) and **9** (B) in inactin-anesthetized rats (n = 3). PEG-400 was used as vehicle. The plasma drug levels at the end of the study for both compounds are comparable (72 and 80 μg/mL, respectively, for **5c** and **9**, see Table 1).

in methylene chloride. Triethylamine (excess, 2 mL) and acetic anhydride (excess, 1 mL) were added sequentially at room temperature, and the mixture was stirred for 0.5 h. After the removal

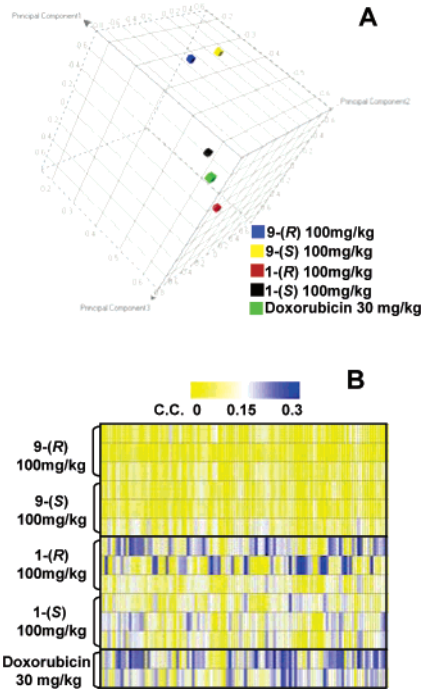

Figure 3. Gene expression analysis of rat heart. The rats were dosed orally (1% Tween in water as vehicle) at 100 mg/kg (bid) for 3 days and heart tissues were harvested for microarray analysis. Doxorubicin was used as a positive control. The results were compared with Iconix *DrugMatrix* database. (A) Principle component analysis of gene expression profiles resulting from treatment with **9**-(*S*), **9**-(*R*), **1**-(*S*), **1**-(*R*), and doxorubicin. The three principal components were generated and plotted for each compound using Spotfire software. Each color point represents a drug treatment. (B) Correlation of heart gene expression changes from rats treated with **9**-(*S*), **9**-(*R*), **1**-(*S*), **1**-(*R*), and doxorubicin with heart gene expression profiles of known cardiac toxicants within *DrugMatrix*. Each row represents a single animal treatment (n = 3) and each column a reference expression profile in *DrugMatrix*. C.C. = correlation coefficient.

of solvent, the residue was purified on a silica gel flash column, eluting with 35∼100% ethyl acetate in hexane, to provide 2.34 g of **9** (74%). ^{1}H NMR (500 MHz, DMSO-d_6) δ ppm 8.48 (d, J = 7.54 Hz, 1H), 7.94 (s, 1H), 7.31−7.36 (m, 2H), 6.99−7.05 (m, 2H), 6.88 (s, 1H), 5.06−5.14 (m, 1H), 4.58−4.67 (m, 1H), 1.87 (s, 3H), 1.43 (d, J = 6.96 Hz, 3H), 1.29 (d, J = 6.38 Hz, 6H); ^{13}C NMR (126 MHz, DMSO-d_6) δ ppm 174.89, 168.65, 155.78, 155.17, 147.96, 139.23, 121.77, 118.79, 116.74, 98.45, 69.74, 41.27, 22.41, 21.70, 18.81. MS (ESI) m/z: 388.0 $(M + H)^+$. Anal. ($C_{19}H_{21}N_3O_4S$) C, H, N, S.

hACC1 and hACC2 Assays. See Supporting Information.

Compound Evaluation in Inactin-Anesthetized Rat Cardiovascular Assay. Male Sprague−Dawley rats (325−375 g) were anesthetized with the long-acting barbiturate, Inactin (100 mg/kg, ip). Catheters (PE-50) were placed in the femoral artery for measurement of mean arterial pressure and heart rate. A specialized transducer tip catheter (Millar Instruments Inc., Houston, TX) was inserted into the left ventricle of the heart for measurement of left ventricular pressure. The index of cardiac contractility dP/dt_{50} was derived from the left ventricular pressure at 50 mmHg. Hemodynamic data was monitored continuously and acquired at 250 Hz at a logging rate of every 5 s, which was averaged every minute using a Ponemah software platform (Gould Instrument Systems, Valley View, OH). Post-hoc, data was further reduced to 5 min averages for each rat using a Microsoft Excel spreadsheet application. Additional catheters were placed in the femoral vein for compound administration (1−2 mL/kg) and saline infusion (10 μL/min) to maintain hydration. Escalating doses were given in half log increments, such that the complete dose was administered by the end of each 30 min infusion period. The highest dose infused was

45 mg/kg. The compounds were dosed using poly(ethylene glycol) 400 (PEG-400) as the vehicle. The cardiac contractility results are expressed as mean ± SEM ($n = 3$ rats per compound).

Gene Expression Analysis. Male Sprague−Dawley rats [Crl: CD(SD)IGS BR] weighing approximately 200∼250 g were obtained from Charles River Laboratories, Inc., Portage, MI. The animals were treated with 100 mg/kg **9**-(*S*) (active), **9**-(*R*) (inactive), **1**-(*S*) (active), and **1**-(*R*) (inactive) twice daily (b.i.d) by oral gavage for a period of 3 days and sacrificed on day 4. Vehicle control was H_2O containing 1% Tween. The hearts were snap-frozen in liquid nitrogen for RNA isolation. Experiments were performed according to the guidelines established in the National Institutes of Health Guide for the Care and Use of Laboratory Animals. Frozen heart samples were immediately added to TRIzol reagent (Invitrogen Life Technologies, Carlsbad, CA) and homogenized using a Polytron 300D homogenizer (Brinkman Instruments, Westbury, NY). One mL of the tissue homogenate was transferred to a microfuge tube, and total RNA was isolated from the TRIzol extracts following the standard protocol provided by the manufacturer (Invitrogen Life Technologies, Carlsbad, CA). The quality of total RNA was monitored using the RNA 6000 Nano Assay with the 2100 Agilent Bioanalyzer (Agilent Technologies, Palo Alto, CA). The microarray experiment was performed on Affymetrix RAE230A GeneChip according to the manufacturer's protocol, with the exception that the primer used for the reverse transcription reaction was the GeneChip T7-Oligo(T) Promoter Primer Kit (Affymetrix, Santa Clara, CA).

The microarray scanned image and intensity files were imported into Rosetta Resolver gene expression analysis software version 5.0 (Rosetta Inpharmatics, Seattle, WA). Resolver's Affymetrix error model was applied, and ratios were built for each treatment versus the vehicle controls. Principal components analysis was completed using Spotfire Decision Site version 8.0 (Spotfire, Somerville, MA). The similarity of gene expression profiles of the test compound and reference compounds from the *DrugMatrix* database (Iconix Pharmaceuticals, Mountain View, CA) was calculated as the Pearson's correlation coefficient based on the common genes shared by the Affymetrix RAE230A and Codelink RU1 (GE Healthcare, Piscataway, NJ).

Acknowledgment. We thank Dr. Xiaolin Zhang, Andy L. Adler, and Todd N. Turner for technical support.

Supporting Information Available: Synthetic procedures, analytical and spectroscopic data of the new compounds and key intermediates in Table 1, as well as **9**-(*S*) and **9**-(*R*), detailed protocol of human ACC1 and ACC2 assays, pharmacokinetic data of compounds **1**-(±), **9**-(±), **9**-(*S*), and **9**-(*R*). This material is available free of charge via the Internet at http://pubs.acs.org.

References

(1) Turkoglu, C.; Duman, B. S.; Gunay, D.; Cagatay, P.; Ozcan, R.; Buyukdevrim, A. S. Effect of Abdominal Obesity on Insulin Resistence and the Components of the Metabolic Syndrome: Evidence Supporting Obesity as the Central Feature. *Obes. Surg.* **2003**, *13* (5), 699−705.

(2) Steyn, N. P.; Mann, J.; Bennett, P. H.; Temple, N.; Zimmet, P.; Tuomilehto, J.; Lindstrom, J.; Louheranta, A. Diet, Nutrition and the Prevention of Type 2 Diabetes. *Public Health Nutr.* **2004**, *7* (1A), 147−165.

(3) Hulver, M. W.; Berggren, J. R.; Cortright, R. N.; Dudek, R. W.; Thompson, R. P.; Pories, W. J.; MacDonald, K. G.; Cline, G. W.; Shulman, G. I.; Dohm, G. L.; Houmard, J. A. Skeletal Muscle Lipid Metabolism with Obesity. *Am. J. Physiol.:Endocrinol. Metab.* **2003**, *284*, E741−747.

(4) Sinha, R.; Dufour, S.; Petersen, K. F.; LeBon, V.; Enoksson, S.; Ma, Y.-Z.; Savoye, M.; Rothman, D. L.; Shulman, G. I.; Caprio, S. Assessment of Skeletal Muscle Triglyceride Content by ^{1}H Nuclear Magnetic Resonance Spectroscopy in Lean and Obese Adolescents: Relationships to Insulin Sensitivity, Total Body Fat, and Central Adiposity. *Diabetes* **2002**, *51* (1), 1022−1027.

(5) (a) Kusunoki, J.; Kanatani; A.; Moller, D. E. Modulation of Fatty Acid Metabolism As A Potential Approach to the Treatment of Obesity and the Metabolic Syndrome. *Endocrine* **2006**, *29* (1), 91−100.

(6) Munday, M. R.; Hemingway, C. J. The Regulation of Acetyl-CoA Carboxylase-A Potential Target for the Action of Hypolipidemic Agents. *Adv. Enzyme Regul.* **1999**, *39*, 205−234.

(7) Ruderman, N. B.; Saha, A. K.; Vavvas, D.; Witters, L. A. Malonyl-CoA, Fuel Sensing, and Insulin Resistance. *Am. J. Physiol.* **1999**, *276*, E1−E18.

(8) Ruderman, N. B.; Saha, A. K.; Kraegen, E. W. Minireview: Malonyl CoA, AMP-Activated Protein Kinase, and Adiposity. *Endocrinology* **2003**, *144* (12), 5166−5171.

(9) Mao, J.; Chirala, S. S.; Wakil, S. J. Human Acetyl-CoA Carboxylase 1 Gene: Presence of Three Promoters and Heterogeneity at the 5′-Untranslated mRNA Region. *Proc. Natl. Acad. Sci. U.S.A.* **2003**, *100*, 7515−7520.

(10) Abu-Elheiga, L.; Almarza-Ortega, D. B.; Baldini, A.; Wakil, S. J. Human Acetyl-CoA Carboxylase 2, Molecular Cloning, Characterization, Chromosomal Mapping, and Evidence for Two Isoforms. *J. Biol. Chem.* **1997**, *272*, 10669−10677.

(11) Abu-Elheiga, L.; Matzuk, M. M.; Kordari, P.; Oh, W.; Shaikenov, T.; Gu, Z.; Wakil, S. J. Mutant Mice Lacking Acetyl-CoA Carboxylase 1 Are Embryonically Lethal. *Proc. Natl. Acad. Sci. U.S.A.* **2005**, *102* (34), 12011−12016.

(12) Abu-Elheiga, L.; Matzuk, M. M.; Abo-Hashema, K. A. H.; Wakil, S. J. Continuous Fatty Acid Oxidation and Reduced Fat Storage in Mice Lacking Acetyl-CoA Carboxylase 2. *Science* **2001**, *291*, 2613−2616.

(13) Abu-Elheiga, L.; Oh, W.; Kordari, P.; Wakil, S. J. Acetyl-CoA Carboxylase 2 Mutant Mice Are Protected Against Obesity and Diabetes Induced by High-fat/High-carbohydrate Diets. *Proc. Natl. Acad. Sci. U.S.A.* **2003**, *100*, 10207−10212.

(14) Gu, Y. G.; Weitzberg, M.; Clark, R. F.; Xu, X.; Li, Q.; Zhang T.; Hansen, T. M.; Liu, G.; Xin, Z.; Wang, X.; Wang, R.; McNally, T.; Zinker, B. A.; Frevert, E. U.; Camp, H. S.; Beutel, B. A.; Sham, H. L. Synthesis and Structure−Activity Relationships of *N*-{3-[2-(4-Alkoxyphenoxy)thiazol-5-yl]-1-methylprop-2-ynyl}carboxy Derivatives as Selective Acetyl-CoA Carboxylase 2 Inhibitors. *J. Med. Chem.* **2006**, *49* (13), 3770−3773.

(15) Polakowski, J. S.; Segreti, J. A.; Cox, B. F.; Hsieh, G. C.; Kolasa, T.; Moreland, R. B.; Brioni, J. D. Effects of Selective Dopamine Receptor Subtype Agonists on Cardiac Contractility and Regional Haemodynamics in Rats. *Clin. Exp. Pharmacol. Physiol.* **2004**, *31*, 837−841.

(16) Reinhart, G. A.; Fryer, R. M.; Osinski, M. A.; Polakowski, J. S.; Cox, B. F.; Gintant, G. A. Predictive, non-GLP Models of Secondary Pharmacodynamics: Putting the Best Compounds Forward. *Curr. Opin. Chem. Biol.* **2005**, *9*, 1−8.

(17) Kym, P. R.; Souers, A. J.; Campbell, T. J.; Lynch, J. K.; Judd, A. S.; Iyengar, R.; Vasudevan, A.; Gao, J.; Freeman, J. C.; Wodka, D.; Mulhern, M.; Zhao, G.; Wagaw, S. H.; Napier, J. J.; Brodjian, S.; Dayton, B. D.; Reilly, R. M.; Segreti, J. A.; Fryer, R. M.; Preusser, L. C.; Reinhart, G. A.; Hernandez, L.; Marsh, K. C.; Sham, H. L.; Collins, C. A.; Polakowski, J. S. Screening for Cardiovascular Safety: A Structure−Activity Approach for Guiding Lead Selection of Melanin Concentrating Hormone Receptor 1 Antagonists. *J. Med. Chem.* **2006**, *49*, 2339−2352.

(18) Firouzabadi, H.; Sardarian, A. R.; Badparva, H. Highly Selective Amidation of Benzylic Alcohols With Nitriles: A Modified Ritter Reaction. *Synth. Commun.* **1994**, *24* (5), 601−607.

(19) Childs, A. C.; Phaneuf, S. L.; Dirks, A. J.; Phillips, T.; Leeuwenburgh. C. Doxorubicin Treatment In Vivo Causes Cytochrome *c* Release and Cardiomyocyte Apoptosis, as well as Increased Mitochondrial Efficiency, Superoxide Dismutase Activity, and Bcl-2:Bax Ratio. *Cancer Res.* **2002**, *62*, 4592−4598.

(20) Ganter, B.; Tugendreich, S.; Pearson, C. I.; Ayanoglu, E.; Baumhueter, S.; Bostian, K. A.; Brady, L.; Browne, L. J.; Calvin, J. T.; Day, G.-J.; Breckenridge, N.; Dunlea, S.; Eynon, B. P.; Furness, L. M.; Ferng, J.; Fielden, M. R.; Fujimoto, S. Y.; Gong, L.; Hu, C.; Idury, R.; Judo, M. S. B.; Kolaja, K. L.; Lee, M. D.; McSorley, C.; Minor, J. M.; Nair, R. V.; Natsoulis, G.; Nguyen, P.; Nicholson, S. M.; Pham, H.; Roter, A. H.; Sun, D.; Tan, S.; Thode, S.; Tolley, A. M.; Vladimirova, A.; Yang, J.; Zhou, Z.; Jarnagin, K. Development of A Large-scale Chemogenomics Database To Improve Drug Candidate Selection and To Understand Mechanisms of Chemical Toxicity and Action. *J. Biotechnol.* **2005**, *119*, 219−244.

JM070035A